# ELECTROOPTIC AND PHOTOREFRACTIVE PROPERTIES OF IRON-DOPED LITHIUM NIOBATE CRYSTALS WITH EXTERNALLY APPLIED EXTREMELY LARGE ELECTRIC FIELDS[1]

**M. LUENNEMANN, K. PEITHMANN, U. HARTWIG, K. BUSE**

**University of Bonn, Physical Institute**
*(Wegelerstraße 8, D-53115 Bonn, Germany; email: kbuse@uni-bonn.de)*

UDC 535.215


The influence of extremely large, externally applied electric fields onto the electrooptic and photorefractive properties of iron-doped lithium-niobate crystals is investigated using reflection holography. The impact of an active feedback method used for interference fringe stabilization during holographic recording is studied. We show that extremely large fields increase the photorefractive sensitivity $S$ up to 40 cmJ$^{-1}$ and saturation values of the refractive-index changes $\Delta n_s$ to $12 \times 10^{-4}$. Furthermore, the feedback system introduces a frequency shift between the two recording beams and modifies the photorefractive response of the crystals.

Iron-doped lithium-niobate crystals are of substantial interest for applications in many fields of optics, such as holographic data storage [1], integrated optics [2], or telecommunication [3]. In iron-doped, photorefractive lithium-niobate ($LiNbO_3$) crystals light excites electrons from $Fe^{2+}$ sites. The electrons migrate due to the drift in externally applied and internal electric fields, diffusion, and the bulk-photovoltaic effect. Finally, they are caught by $Fe^{3+}$ ions. A space-charge field $E_{SC}$ builds up and changes the refractive index $n$ by the electrooptic effect [4–8]. For no or moderate externally applied electric fields the processes are well known; they can be described using the so-called one-center model [9,10]. For applications, large refractive-index changes $\Delta n$ for small amounts of light are desired. Thus, the photorefractive sensitivity $S$ is an important quality measure, where $S$ is defined as

$$S = \frac{1}{Id}\frac{\partial\sqrt{\eta}}{\partial t} \quad \text{for } t \ll \tau \ , \qquad (1)$$

with $I$ as the light intensity, $d$ as the crystal thickness, $\eta$ as diffraction efficiency, $t$ as time, and $\tau$ is the recording time constant. High $S$ values are required for sensitive recording.

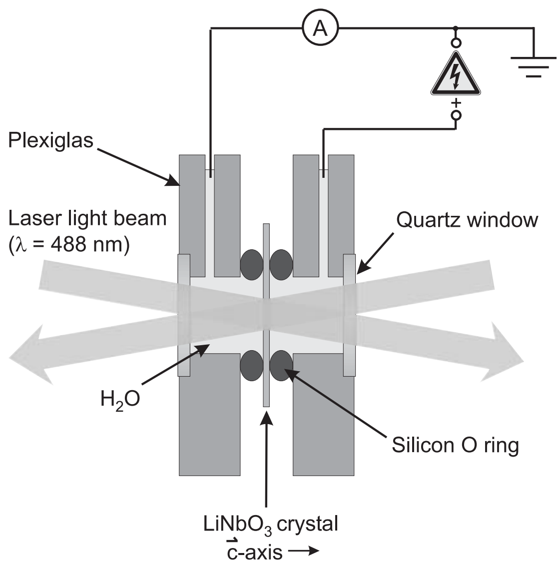


Fig. 1. Schematic illustration of the crystal mount used in our experiments

It is well known that external electric fields yield additional drift currents and hence influence the photorefractive performance. However, it was so far unknown what are the highest fields that can be applied to $LiNbO_3$ crystals and how the material behaves for extremely large fields. The goal is to improve the photorefractive properties significantly.

All our investigations are performed using congruently melting, single-domain, iron-doped $LiNbO_3$ crystals. The iron content covers the range $c_{Fe} = (18-56)\times10^{24}$ m$^{-3}$. The sample size is $10\times10\times0.22$ mm, where the crystalographic $c$ axis is oriented along the 0.22 mm length (so-called $z$-cut geometry). We utilize two plane waves of ordinarily polarized light, emitted by an argon-ion laser at $\lambda = 488$ nm, for our holography experiments. To mount the crystal and to apply large external electric fields, a sample holder illustrated in Fig. 1 is used. The crystal is clamped between two PMMA slabs using silicon O rings; the surfaces are contacted by means of liquid electrodes. Electric fields

[1]This article is dedicated to Professor Marat Soskin on the occasion of his 75th birthday.

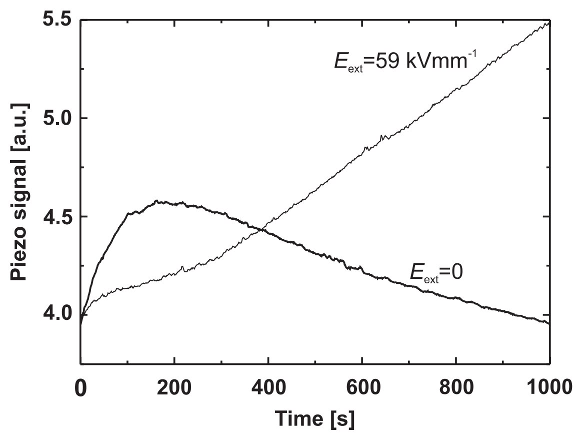


Fig. 2. Voltage applied to the piezoelectrically supported mirror for the utilized active feedback-controlled stabilization system vs time $t$. Two different electric fields have been applied. After some time, a constant drift of the mirror is observed

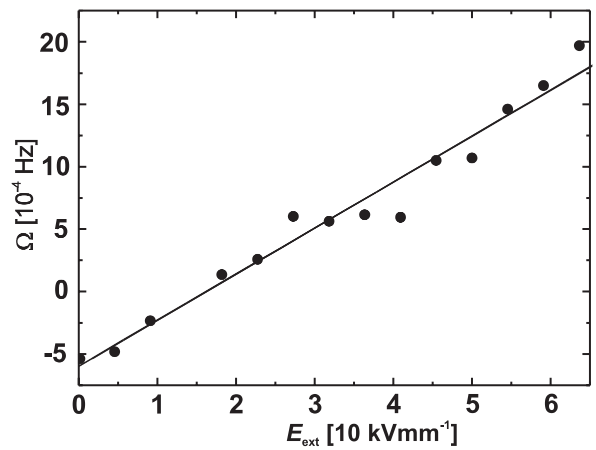


Fig. 3. Frequency detuning of the piezoelectrically supported mirror vs externally applied electric field $E_{\text{ext}}$

up to 65 kVmm$^{-1}$ are applied. Using larger fields ($> 70$ kVmm$^{-1}$) yields electric breakdowns and crystal damage.

The setup is used to record elementary reflection holograms by interference of two plane waves. For subsequent readout of the recorded hologram, just one of the recording beams is used while blocking the second one. The light intensities of the transmitted and diffracted light beams behind the crystal, $I_{\text{T}}$ and $I_{\text{D}}$, allow one to calculate the diffraction efficiency $\eta = I_{\text{D}}/(I_{\text{T}} + I_{\text{D}})$ and thus to obtain the refractive-index amplitude $\Delta n$ [11].

Additionally, we apply an active feedback loop to stabilize the interference pattern against mechanical disturbances [12–14]. This feedback configuration uses beam-coupling signals, obtained by a photodiode in one of the two transmitted recording beams, to correct for shifts in the phase between the light intensity and refractive-index pattern. The phase of the light pattern can be adjusted by a piezoelectrically driven mirror that changes the phase of one of the writing beams.

Using reflection geometry, a significant motion of the piezoelectrically driven mirror during the recording process is observed. We monitor the voltage of the mirror. Fig. 2 shows the voltage measured vs time for two different recording experiments using two different values of the externally applied electric field $E_{\text{ext}}$.

After some time when transient effects have stopped, a constant drift of the mirror is observed. This causes a frequency detuning of the light reflected by the mirror. For no external electric field, a negative value of the detuning is measured; for large fields $E_{\text{ext}}$ positive values are obtained. Fig. 3 shows the frequency detuning plotted for different applied electric fields [14].

The frequency detuning has a linear dependence on $E_{\text{ext}}$. This yields a moving interference pattern and thus a moving space-charge grating. Hence, the stabilization system causes a resonant enhancement of the photorefractive response in the crystal which leads to a maximization of the diffraction efficiency [14].

To check whether we have to consider solely the linear electrooptic effect or if contributions of the quadratic electrooptic effect have to be taken into account at these high external fields, one hologram is recorded and thermally fixed to make it stable against the readout with the writing light wavelength [15, 16]. This hologram is read out for different external electric fields $E_{\text{ext}}$. Changing the field, the Bragg angle under which the hologram has to be read changes, too. Thus the crystal has to be turned by a certain angle $\Delta\Theta_{\text{B}}$ to achieve the best diffraction efficiency. Fig. 4 shows the angular position change $\Delta\Theta_{\text{B}}$ vs $E_{\text{ext}}$. A linear dependence is found within the measurement accuracy. Thus we conclude that we can neglect any influence of the quadratic electrooptic effect, because a non-linear behaviour of $\Delta\Theta_{\text{B}}$ with increasing $E_{\text{ext}}$ must be present otherwise [17].

Finally, we measure the photorefractive properties with externally applied fields. In particular, we investigate three crystals with the same iron content ($c_{\text{Fe}} = 56\times10^{24}$ m$^{-3}$), but different ratios of filled ($Fe^{2+}$) and empty ($Fe^{3+}$) traps, $c_{\text{Fe}^{2+}}/c_{\text{Fe}^{3+}}$. First, we measure

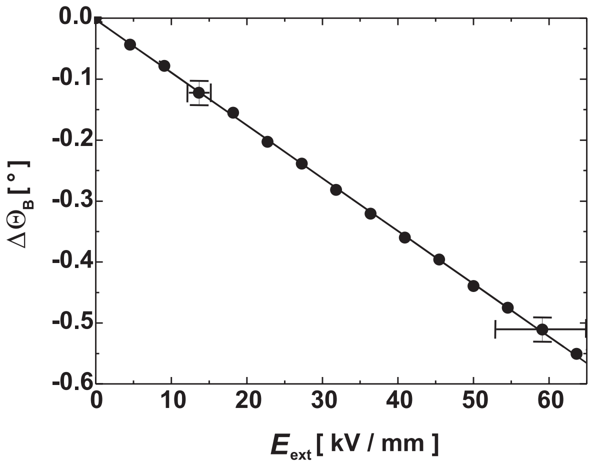


Fig. 4. Change of the readout Bragg angle $\Delta\Theta_B$ vs externally applied electric field $E_{ext}$ for a thermally fixed reflection hologram

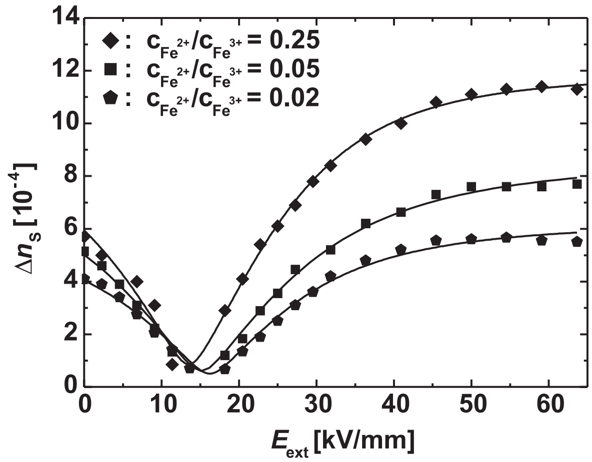


Fig. 5. Saturation values of the refractive-index changes $\Delta n_s$ vs externally applied field $E_{ext}$. The symbols represent experimental data; the lines are fits using the standard one-center model equations [9,10,17]

the saturation values of the refractive-index changes $\Delta n_s$ for various fields $E_{ext}$. The result is shown in Fig. 5 [18].

After going through a minimum, values of up to almost $12 \times 10^{-4}$ are obtained. The $\Delta n_s$ values with large field are considerably larger compared to that at zero field. However, for very large $E_{ext}$, the values for $\Delta n_s$ saturate. The minimum of the $\Delta n_s(E_{ext})$ curves indicates the bulk-photovoltaic (PV) field $E_{PV}$ [10]: Here, $E_{PV}$ is cancelled by the field $E_{ext}$, and the remaining effect is quite small, dominated by diffusion.

Fig. 6 shows the sensitivity $S$ for different concentration ratios $c_{Fe^{2+}}/c_{Fe^{3+}}$. We find that $S$ grows strongly; the best values approach $S = 40$ cmJ$^{-1}$. For very large fields $E_{ext}$ the sensitivity is still growing. In general, samples that have been reduced (large $c_{Fe^{2+}}/c_{Fe^{3+}}$ ratio) show a higher sensitivity. Again, a minimum in the case of $E_{PV} = E_{ext}$ is obvious.

Our results show: External electric fields of up to 65 kVmm$^{-1}$ can be applied to $LiNbO_3$ crystals. Writing reflection holograms in an efficient way utilizing a feedback-controlled active stabilization system is feasible. The feedback loop introduces a frequency shift which is determined by the externally applied electric field $E_{ext}$. Any impact of the quadratic electrooptic effect does not have to be considered.

The values for the refractive-index changes $\Delta n_s$ can be improved up to $12 \times 10^{-4}$. Without field, the best value is $7 \times 10^{-4}$ [19]. It is possible to understand this phenomena taking the well-known one-center model and its equations [9,10,17] to describe the data, as indicated by the lines in Fig. 5:

$$E_{SC} = -\frac{E_{ext} + E_{PV} + iE_D}{1 + \frac{E_D}{E_q} - \frac{iE_{ext}}{E_q} - \frac{iE_{PV}}{E'_q}} \quad (2)$$

with $E_{PV} = j_{PV}/\sigma_{ph}$ as the bulk-photovoltaic field defined by the bulk-photovoltaic current density $j_{PV}$ and the photoconductivity $\sigma_{ph}$, $E_D = k_B T K/e$ as the diffusion field with $K$ as the grating vector, and with $E_q = e/(\epsilon\epsilon_0 K)(1/c_{Fe^{2+}} + 1/c_{Fe^{3+}})^{-1}$ and $E'_q = e/(\epsilon\epsilon_0 K)c_{Fe^{2+}}$ as the space-charge limiting fields. For very large external fields $E_{ext}$ the equations yield $E_{SC} = -E_q$, with $E_q$ representing the space-charge field limiting field. Thus, for increasing field, the values for $E_{SC}$ and thus for $\Delta n_s$ reach a saturation level.

In a similar way, the sensitivity $S$ for different applied fields can be understood. Fig. 6 contains the fit curves, obtained with the use of the one-center model, as the solid lines:

$$S = a[(E_{ext} + E_{PV})^2 + E_D^2]^{1/2} \ , \quad (3)$$

$$a = \frac{\pi n_o^3 r_{113}}{2I\lambda \cos\theta\tau} \ , \quad (4)$$

with $n_o$ as the refractive index for ordinarily polarized light, $r_{113}$ as the electrooptic coefficient, $\lambda$ as the light wavelength, and $\theta$ as the anlge between the light beam and the surface normal of the crystal. The model describes the measured data in a very convincing manner. However, in contrast to $\Delta n_s$, the sensitivity $S$

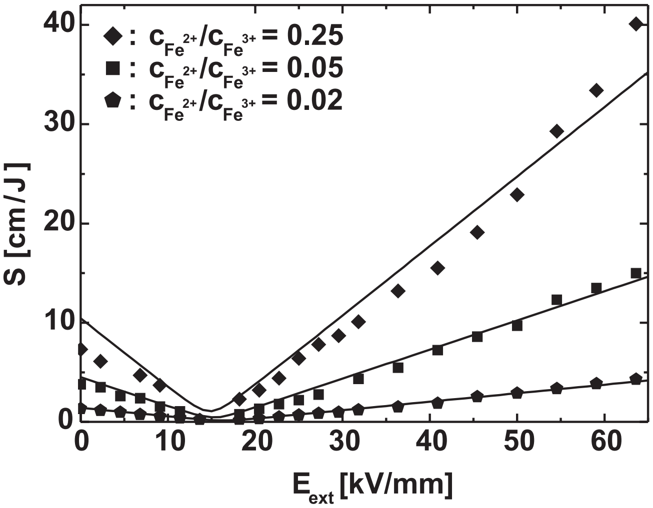


Fig. 6. Sensitivity $S$ vs externally applied field $E_{\rm ext}$. The symbols represent experimental data; the lines are fits using the standard one-center model equations [9, 10, 17]

is not limited; larger fields increase $S$. For very large values for $E_{\rm ext}$, we get $S \propto E_{\rm ext}$, which agrees with the experimentally found facts. Our value of $S = 40$ cmJ$^{-1}$ exceeds the best values obtained without field by a factor of 4.

In conclusion, the application of very large external electric fields to $LiNbO_3$ doped with iron is a very promising way to provide a holographic storage material with a large dynamic range and sufficient sensitivity.

We thank G. Panotopoulos and B. Sturman for valuable cooperation and discussions.

This work was supported the Deutsche Forschungsgemeinschaft, Germany, and the Deutsche Telekom AG, Germany.

1. *Springer* Series in Optical Sciences/ Ed. by H.J. Coufal, D. Psaltis, D. von der Linde, T.J. Negran. — Berlin: Springer, 2000.
2. *Becker C., Greiner A., Oesselke T. et al.* // Opt. Lett. — 1998. — **23**. — P.1194—1196.
3. *Springer* Series in Optical Sciences/ Ed. by P. Boffi, D. Piccinin, M.C. Ubaldi. — Berlin: Springer, 2003.
4. *Chen F.S., LaMacchia J.T., Fraser D.B.* // Appl. Phys. Lett. — 1968. — **25**. — P.223—225.
5. *Kurz H., Krätzig E., Keune W. et al.* // Appl. Phys. — 1977. — **12**. — P.355—368.
6. *Buse K.* // Appl. Phys. B. — 1997. — **64**. — P.273—291.
7. *Buse K.* //Ibid. — **64**. — P.391—407.
8. *Glass A.M., von der Linde D., Negran T.J.* // Appl. Phys. Lett. — 1974. — **25**. — P.233—235.
9. *Kukhtarev N.V.* // Sov. Phys. Tech. Lett. — 1976. — **2**. — P.438—440.
10. *Kukhtarev N.V., Markov V.B., Odoulov S.G. et al.* // Ferroelectrics. — 1979. — **22**. — P.949—960, 961—964.
11. *Kogelnik H.* // Bell System Techn. J. — 1969 — **48**. — P.2909—2947.
12. *DosSantos P.A.M., Cescato L., Frejlich J.* // Opt. Lett. — 1988. — **13**. — P.1014—1016.
13. *Garcia P.M., Buse K., Kip D., Frejlich J.* // Opt. Communs. — 1995. — **117**. — P.235—240.
14. *Luennemann M., Buse K., Sturman, B.* //J. Appl. Phys. — 2003. — **94**. — P.6274—6279.
15. *Amodei J.J., Staebler D.L.* // Appl. Phys. Lett. — 1971. — **18**. — P.540—542.
16. *Buse K., Breer S., Peithmann K. et al.* // Phys. Rev. B. —1997.— **56**.— P.1225— 1235.
17. *Luennemann M., Hartwig U., Panotopulous G., Buse K.* //Ibid. —2003.— **76**.— P.403 — 406.
18. *Luennemann M., Hartwig U., Buse, K.* // J. Opt. Soc. B. — 2003. — **20**. — P.1643—1648.
19. *Peithmann K., Wiebrock A., Buse K.* // Appl. Phys. B. — 2003. — **68**. — P.777—784.

ЕЛЕКТРООПТИЧНІ ТА ФОТОРЕФРАКТИВНІ ВЛАСТИВОСТІ КРИСТАЛІВ НІОБАТУ ЛІТІЮ З ДОМІШКОЮ ЗАЛІЗА В НАДПОТУЖНИХ ЗОВНІШНІХ ЕЛЕКТРИЧНИХ ПОЛЯХ

*М. Люннеман, К. Пайтман, У. Хартвіг, К. Бузе*

Р е з ю м е

Вплив надпотужних зовнішніх електричних полів на електрооптичні та фоторефрактивні властивості кристалів ніобату літію, легованих залізом, досліджено за допомогою запису відбивних голограм. Вивчено вплив методу активного зворотного зв'язку, який було використано для стабілізації інтерференційної картини під час голографічного запису. Показано, що надпотужні електричні поля збільшують фоторефрактивну чутливість $S$ до 40 см· Дж$^{-1}$, а значення насичення зміни показників заломлення $\Delta n_{\rm s}$ — до $12 \times 10^{-4}$. Окрім того, система зворотного зв'язку вносить частотний збій між двома записуючими променями та змінює фоторефрактивний відгук даних кристалів.